Conductance measurements on P_b centers at the (111) $Si:SiO_2$ interface

M. J. Uren[a)]
Defence Research Agency, Great Malvern, Worcestershire WR14 3PS, United Kingdom

J. H. Stathis and E. Cartier
IBM Research Division, T J Watson Research Center, Yorktown Heights, New York 10598

(Received 5 April 1996; accepted for publication 25 June 1996)

The electrical properties of the P_b center have been measured using the conductance technique over the temperature range 130–290 K. A high concentration of P_b centers was created by vacuum annealing of 28-nm-thick thermal oxides on (111) silicon surfaces. Fitting the conductance data allowed the contribution of the $(0/-)$ P_b level to be separated from the U-shaped background states. The $(0/-)$ peak in the density of states was found to be asymmetrical with a broad shoulder on the conduction band side. The P_b levels were found to show a capture cross section which fell toward the band edges and which could be fitted by assuming an activated cross section with an activation energy which increased toward the band edges. By contrast, the background states showed a cross section which was temperature and band bending independent. [S0021-8979(96)02119-6]

I. INTRODUCTION

Interface states at the $Si:SiO_2$ surface have been studied in exhaustive detail because of their effect on the reliability and capability of the silicon metal–oxide–silicon (MOS) field-effect transistor. Despite this enormous effort, very little is understood about their microscopic structure or formation mechanism.[1] The only exception is the P_b center which has become the archetypal interface state. Extensive measurements carried out using electron paramagnetic resonance (EPR) and capacitance–voltage (C–V) measurements have conclusively identified this defect as a dangling bond on a silicon atom at the $Si:SiO_2$ interface.[2–4] On the (111) surface, the dangling bond axis is perpendicular to the $Si:SiO_2$ surface and it is a positive U amphoteric defect, i.e., it can have three charge states (positive, neutral, or negative) accepting either one or two electrons. The energy levels above the valence-band edge are found to be 0.27 eV for the $(+/0)$ and 0.83 eV for the $(0/-)$ levels. Many studies have been carried out over the years, both theoretical[5,6] and experimental,[7–10] which have extended the understanding of the chemistry and annealing of the defect. Despite its importance as the only unambiguously identified interface defect, there have been remarkably few detailed electrical studies carried out. Most work has concentrated on the EPR measurement with largely only C–V carried out to date. The original work on the dangling bond was carried out using deep level transient spectroscopy,[2] but no cross-section information was published. It is increasingly apparent that the dangling bond is only responsible for a part of the defect generation process,[11] but despite that it still remains of great interest.

Here we report the first detailed electrical measurements of the dangling bond level at the (111) Si/SiO_2 interface using the conductance technique.[12] The conductance technique is relatively slow, but gives clear information on properties such as cross-section and level distributions, in some circumstances allowing the separation of different types of interface defect.[13–15] The P_b centers were prepared using vacuum annealing of thermal oxides. This has proved to be a particularly effective approach to the generation of P_b centers because it generates almost exclusively this particular state with very little contamination from other defects.[11] Unlike radiation damage or negative bias stress, almost no slow states were generated by this preparation technique.[15,16]

II. SAMPLE AND EXPERIMENTAL DETAILS

The thermally grown oxides described in this article were grown at IBM Yorktown Heights and are similar to those described elsewhere.[9] The thermal oxides of thickness 28 nm were grown at 900 °C in dry oxygen on n- and p-type (111) silicon wafers of doping 1.5×10^{22} and 1.1×10^{21} m^{-3}, respectively. Vacuum annealing was then carried out at 700 °C for 2 h at a pressure of 1×10^{-6} Torr to fully depassivate the dangling bonds, resulting in a high concentration of silicon dangling bond (P_b) centers as measured using EPR. Since the defects start to anneal at temperatures above 150 °C, all sample preparation was carried out at room temperature. MOS capacitors were fabricated by evaporation of aluminium dots of area 5.5×10^{-7} m^2 through a shadow mask to form the gate, and the back contact was made by abrasion followed by evaporation of aluminium. This made a satisfactory back contact to the n-type samples but resulted in a leaky, relatively high-resistance Schottky contact to the p-type devices which limited their usefulness.

III. HIGH-/LOW-FREQUENCY C–V MEASUREMENTS

The high-/low-frequency C–V measurements were carried out using conventional instrumentation based on a HP4140B picoammeter/voltage source for the quasistatic sweep (QS) and a HP4192A impedance analyzer for the high-frequency measurements.[17] Figure 1 shows the results of 1 MHz C–V and a quasistatic C–V sweep for an n-type sample and are entirely consistent with previous measurements.[2,3,11] The two broad peak structures on either

[a)]Electronic mail: mju@dra.hmg.gb

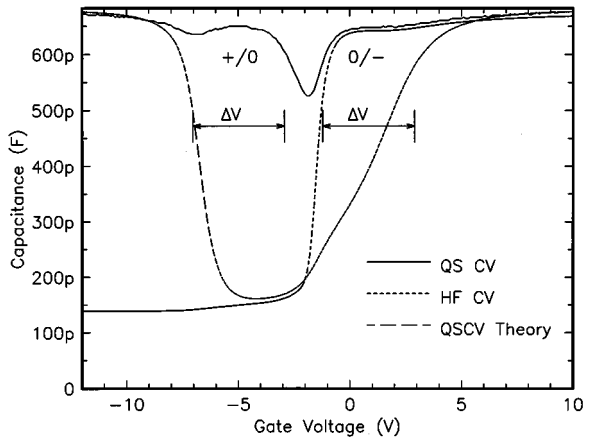

FIG. 1. High-/low-frequency $C-V$ measurement of an n-type MOS capacitor. The voltage extent of the two P_b levels is indicated by the arrows. The long-dashed line shows the theoretical quasistatic curve for a capacitor without interface states.

side of the central dip represent the contribution from the upper and lower levels of the P_b center. In such a $C-V$ measurement, the measured capacitance C_M is given by

$$\frac{1}{C_M}=\frac{1}{C_{\rm ox}}+\frac{1}{C_s+C_T}, \tag{1}$$

where $C_{\rm ox}$, C_s, and C_T are the oxide, silicon and trap capacitances, respectively. C_M is only slightly less than $C_{\rm ox}$ at the trap peaks, which means that C_T is up to 20–30 times greater than $C_{\rm ox}$. Because the extraction of the interface state density ($D_{\rm IT}=C_T/q$) using Eq. (1) relies on an accurate estimate of $C_{\rm ox}$, large errors in inferred $D_{\rm IT}$ will result from any error in $C_{\rm ox}$. In this case, the oxide capacitance was found by using a theoretical value of the silicon capacitance in accumulation to correct the measured accumulation capacitance.[18]

Because the trap capacitance is much higher than the oxide and silicon capacitances, the number of traps can be very simply estimated from the gate voltage width of the peak as indicated in Fig. 1. The number of traps per unit area N_T is just $C_{\rm ox}\Delta V_G/q$ and was found to be 3.5×10^{16} m^{-2}. (This is in reasonable agreement with the number of traps inferred by integrating under the density of states curve from the conductance technique where 3.7×10^{16} m^{-2} was found.)

The band bending as a function of gate voltage has been extracted by integration of the QS data using

$$E-E_i=\text{const}+q\int_{V_{G0}}^{V_G}\left(1-\frac{C_M(V_G)}{C_{\rm ox}}\right)dV_G, \tag{2}$$

with the integration constant being set by using the high-frequency capacitance at midgap assuming uniform doping.[12] (This gives a value for the midgap voltage within 30 mV of that obtained by assuming that the band bending is symmetrical about midgap.[18]) E_i is the intrinsic (midgap) Gibbs free energy at the surface. To extract useful information from the conductance measurements, it is essential to evaluate the band bending as a function of temperature and we discuss this first. Figure 2 shows the quasistatic capacitance in the vicinity of the upper peak for three temperatures

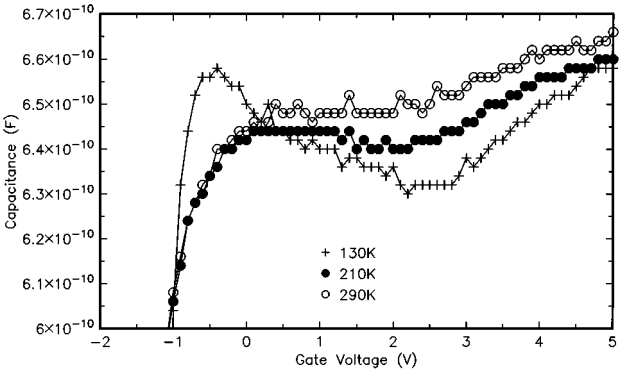

FIG. 2. The portion of the low-frequency (quasistatic) $C-V$ measurement in the vicinity of the $(0/-)$ peak for an n-type capacitor at the indicated temperatures.

where it can be seen that the $C-V$ peak became more clearly defined as the temperature was reduced. As the temperature was reduced, the silicon and trap response times increased so the sweep remained in equilibrium over a smaller and smaller gate voltage range in depletion. In fact, at 130 K the curve was not in equilibrium at voltages below 0.5 V. To carry out the integration of Eq. (2), a reference point was required because midgap could not be accurately identified at the lowest temperatures. Here it was assumed that the trap energy level did not shift with reducing temperature, accordingly, the integration constant at each temperature was evaluated using the room temperature value of $E-E_i=0.31$ eV at $V_G=1$ V. This means that any temperature-dependent shift in the trap energy level will be removed. However, the good overlap of the temperature-dependent QS $C-V$ curves over the range that they were in equilibrium suggests that this effect is small if it exists at all. Figure 3 shows the gate voltage dependence of band bending for the same three temperatures. The arrow indicates the fixed point at the trap peak. It can be seen that there was some temperature dependence to the band bending. As in Fig. 2, the 130 K curve is out of equilibrium below a gate voltage of 0.5 V.

When these band bendings are used to display the density of interface states as a function of temperature (Fig. 4), it

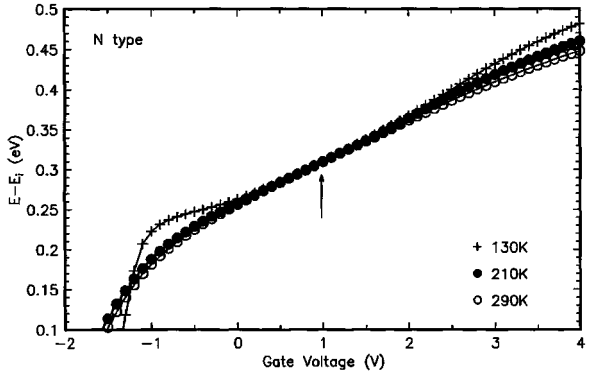

FIG. 3. The surface Fermi energy vs capacitor gate voltage extracted from the data of Fig. 2. The arrow indicates the $(0/-)$ peak position where the curves are offset to have a common value.

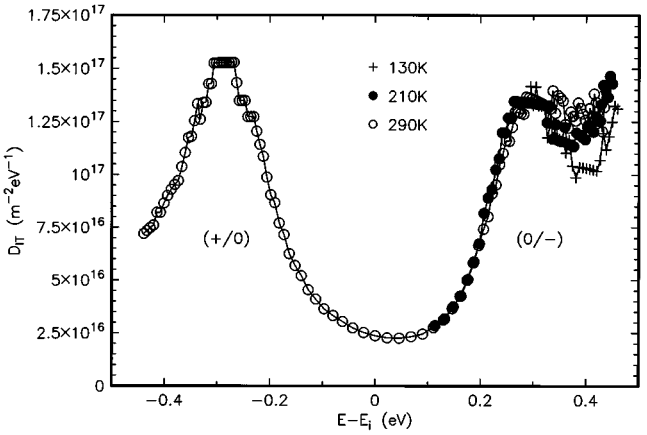

FIG. 4. Density of interface states inferred from the temperature dependent quasistatic $C-V$ curves of Fig. 2.

is clear that the peak due to the $(0/-)$ level became more sharply defined and distinct from the rise toward the conduction-band edge as the temperature was reduced. There did not appear to be any obvious redistribution of states into the peak as the temperature was reduced, rather, the density of states between the peak and the conduction-band edge fell, perhaps representing a redistribution toward the conduction-band edge.

IV. CONDUCTANCE MEASUREMENTS

The conductance technique was used to extract the detailed trap parameters. This technique has excellent resolution and is described in Nicollian and Brews's book in enormous detail.[12] In this particular case, we used a custom-designed bridge which allowed measurements to be made on packaged devices over a frequency range from 1 to 10^7 Hz and at variable temperatures.[19] The equivalent parallel silicon conductance G_P, from which the interface state density can be extracted, is shown in the equivalent circuit shown in the inset to Fig. 5. G_P is related to the measured conductance and capacitance G_M and C_M of a MOS capacitor in depletion by

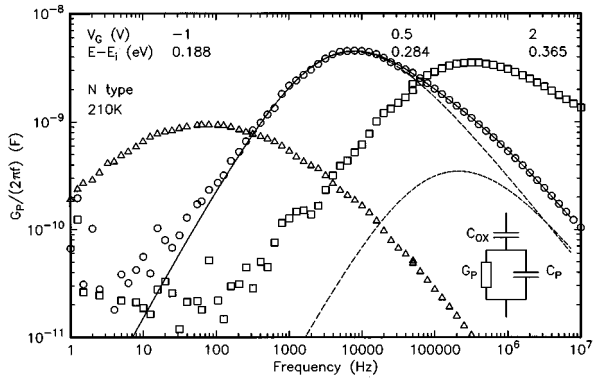

FIG. 5. Equivalent parallel silicon conductance on an n-type capacitor at 210 K for the indicated gate voltages. The solid line shows the result of a five parameter fit to the peak at 0.5 V. The dashed lines show the two peaks that make up that fit.

$$\frac{G_P}{\omega}=\frac{C_{\rm ox}^2 G_M/\omega}{(G_M/\omega)^2+(C_{\rm ox}-C_M)^2}, \tag{3}$$

where $C_{\rm ox}$ is normally taken to be the capacitance in strong accumulation. In this particular case, as for the QS $C-V$ measurement, this was not sufficiently accurate because C_M was so similar to $C_{\rm ox}$. As an indication, for the n-type data using a value for $C_{\rm ox}$ which was corrected for the finite silicon capacitance in accumulation, the density of states reduced at the trap level by 20%. It is very clear that all measurements on these high interface trap densities are potentially very prone to systematic error.

Figure 5 shows the measured conductance versus frequency for three gate voltages at 210 K for an n-type sample in depletion. This temperature was chosen for the figure because it allows conductance curves to be displayed with energies which span the peak in the density of states. As the gate voltage was increased, the Fermi energy moved through the peak closer to the conduction band and the response moved to higher and higher frequency. At higher and lower temperatures, only the lower- or higher-energy side of the defect level could be observed due to the strongly activated nature of the conductance peak frequency. A much more noisy signal was obtained for the p-type sample due to the poor back contact and so the peak shape could not be reliably determined, although the peak frequency could be determined by inspection allowing capture cross-section information to be extracted. In all cases the number of slow states was too low to measure (in contrast to damaged samples where the number can be comparable to the fast state density[16]).

The shape of the conductance peak gives important information about the defect environment. The accepted model for most interface states is that there is a continuum of levels throughout the gap.[12] This is not obviously true for a P_b level which might perhaps be expected to behave rather more like a discrete level. However, it was found that the conductance peak was broadened and could be fitted very well using the continuum model with contributions from two different defects having different characteristic capture cross sections but the same broadening. [Two different cross sections have also been observed on the (100) surface following irradiation.[14,15]] An example of the decomposition is shown in Fig. 5 (this figure shows almost a worst case since for most measurements the relative numbers of the two different cross-section defects were more nearly equal). The fitting was carried out using a nonlinear least-squares-fitting procedure using an approximate form of the continuum model.[20] To cover the full range of conductance peak broadening observed, additional coefficients were needed and these are described in the Appendix. The smaller contribution to the density of states was always found on the higher-frequency side of the conductance peak and represented up to 20% of the total density of states. For energies below $E-E_i=0.22$ eV, the conductance peak broadened so that two contributions could not be separated. The density of states for both contributions is shown in Fig. 6 for all the temperatures measured. The smaller density contribution increased gradually toward the band edge with the larger contribution being due to the

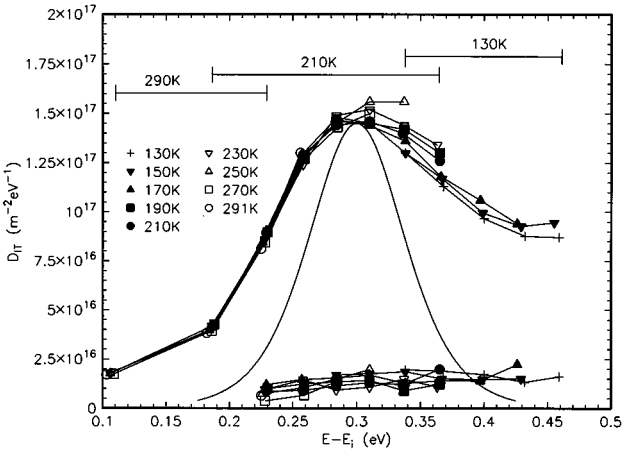

FIG. 6. Density of interface states for the two types of defect separated by the conductance technique. The solid line shows a Fermi derivative function at 290 K to show the maximum width of a discrete level.

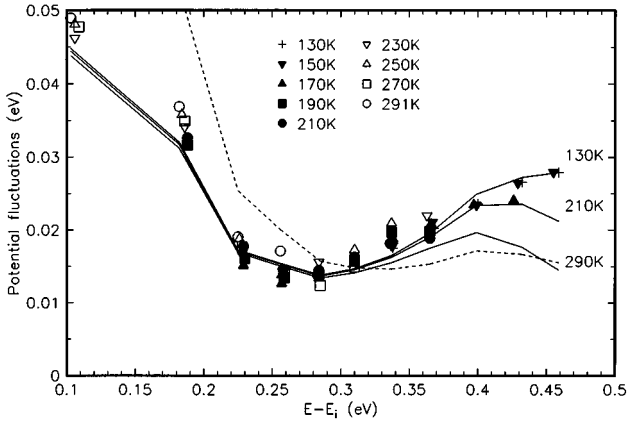

FIG. 7. The standard deviation of the surface potential fluctuations extracted from the width of the conductance peaks. The solid lines show fits to the expression of Eq. (4) at the indicated temperatures with $\gamma = 20$ nm, $N_f^+ + N_f^- = 1.5 \times 10^{16}\ \mathrm{m}^{-2}$ assuming a (0/−) level. The dashed line shows the result of assuming a (+/0) level at 130 K with the same λ and $N_f^+ + N_f^-$.

P_b level. At the top of the figure, the range in energy where the conductance peak could be observed has been shown at three indicative temperatures. Although different parts of the P_b D_{IT} peak are accessible at different temperatures, it seems clear that there was no strong dependence on the density-of-states peak width, with the largest temperature dependence occurring between the peak and the conduction-band edge. A Fermi derivative (which represents the maximum energy resolution possible[21]) for room temperature has been superimposed on the curve so that it can be seen that the D_{IT} peak was considerably wider than a simple discrete level. The magnitude of the density of states at the D_{IT} peak agrees to within about 20% between the QS and conductance techniques (Figs. 4 and 6).

In the continuum model of conductance peaks, the broadening of the peak is attributed to potential fluctuations due to a random distribution of charge across the surface. This local fluctuation in potential will result in a variation in emission energy to the band edge and hence a variation in the trap characteristic time constant leading to a broadening of the conductance peak. The conductance peak broadening parameter is known as σ_s and is the standard deviation of the surface potential in units of k_BT/q. The width of the conductance peak was extracted during the fitting procedure, where it was assumed that both contributions to the density of states saw the same potential fluctuations and hence had the same value of σ_s. As might be expected, the peak width σ_s became wider with decreasing temperature, but less obviously the peak width showed a minimum at the P_b trap energy level (this effect can be seen in the three gate voltages in Fig. 5 which span the trap level). In Fig. 7 the standard deviation of the potential fluctuations ($\sigma_s k_BT/q$) has been plotted as a function of energy. The data now fall on a common curve which is essentially independent of temperature. Brews has produced a simple formula for σ_s based on a three-dimensional treatment of a Poisson distribution of charges at the surface,[12]

$$\sigma_s^2 = \frac{N_f^+ + N_f^- + N_T}{N_0} \ln\left[1 + \left(\frac{C_\lambda}{C_s + C_{\mathrm{ox}} + C_T}\right)^2\right], \tag{4}$$

where N_f^+ and N_f^- are the densities of fixed positive and negative charges, $N_0 = 4\pi[(\epsilon_S + \epsilon_{\mathrm{ox}})\epsilon_0/\beta q]^2$ and $C_\lambda = (\epsilon_S + \epsilon_{\mathrm{ox}})\epsilon_0/\lambda$. λ is a fitting parameter representing a minimum screening length and in previous work has been found to have values between 7.5 and 20 nm. This expression very naturally explains the minimum in σ_s at the D_{IT} peak since at that energy the trap capacitance will be at a maximum. The dependence of σ_s on energy depends on the nature of the trap. If the level were an acceptor (0/−), as is expected for the upper P_b level, then as the Fermi energy moved toward the conduction band, the number of trapped charges N_T would increase; conversely, if the level were a donor (+/0) then the number of trapped charges would decrease. In Fig. 7 both cases have been plotted where it was found that a value of λ of 20 nm was necessary to obtain reasonable agreement. It is quite clear that the normal assumption of an acceptor level gives remarkable good agreement. The density of fixed charge ($N_f^+ + N_f^-$) necessary to explain the results was $1.5\times10^{16}\ \mathrm{m}^{-2}$ which is comparable to the measured positive fixed charge at midgap of $1.1\times10^{16}\ \mathrm{m}^{-2}$ assuming no compensation.

The conductance technique can be used to obtain equilibrium capture kinetics information. The trap capture cross section (for the 0/− level) is approximately given by

$$\sigma \approx \frac{1}{A\tau T^2} \exp\left(\frac{(E_G/2) - (E - E_i)}{k_BT}\right), \tag{5}$$

where τ is the trap time constant which is given by the conductance peak frequency $C/f_{\max}$ with C being a constant related to the potential fluctuations, normally around 2, A is about $6.1\times10^{25}\ \mathrm{m}^{-2}\,\mathrm{s}^{-1}\,\mathrm{K}^{-2}$, $E - E_i$ is the Fermi energy (Gibbs free energy) difference from the intrinsic level, and E_G is the band-gap energy. Any trap degeneracy change has been ignored. There are many sources of systematic error in cross-section measurements and so the absolute value is often only accurate to about an order of magnitude.[12] Figure 8

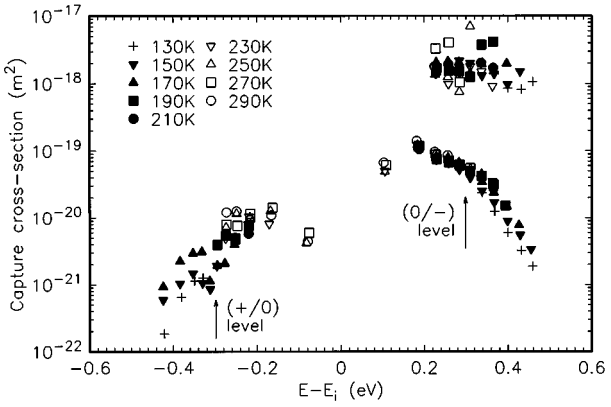

FIG. 8. Capture cross-section of both n- and p-type defects from the conductance measurements. The lower cross-section data in the upper half of the gap corresponds to the P_b level. The arrows indicate the two peaks in the P_b density of states. The trap level temperature dependence was pinned to the nearest band edge.

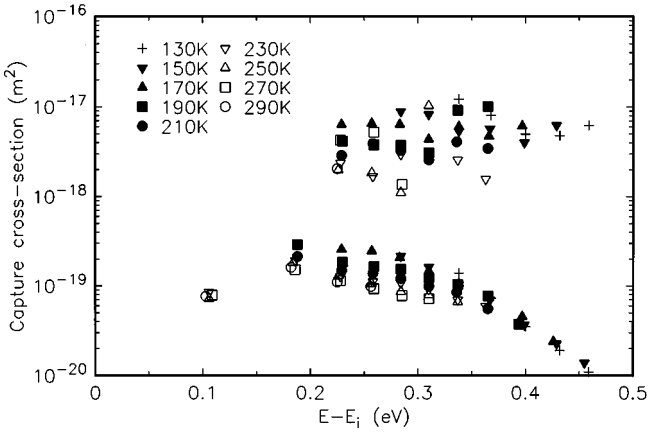

FIG. 9. Capture cross section for the n-type sample as in Fig. 8, but with the trap level temperature dependence pinned to the midgap level.

gives the capture cross section versus energy for both n- and p-type samples. It should be noted that the temperature dependence of the band gap[17] has been ignored and so E_G has been simply set to 1.12 eV (this point will be discussed further). For the n-type sample, the cross section for both types of trap has been shown with the lower cross section being due to the P_b level.

Since the Fermi level enters exponentially into the determination of σ, there is always considerable uncertainty in the absolute value, particularly on the band-edge side of each P_b level. There have been several reports in the past of the cross section falling toward the band edge, however others have found to the contrary (see Nicollian and Brews, p. 314, and Refs. 21 and 22 for a discussion). Here we can be quite definite that the fall in the cross section for the P_b $(0/-)$ level toward the conduction-band edge, which can be observed in Fig. 8, was real and was not an experimental artefact. First, the cross section for the second defect in the upper half of the gap did not fall as the band edge was approached and hence there was a genuine difference apparent. Second, for the cross section to fall, a systematic error in band bending would be required which would result in a stretchout of the curves in Fig. 3. Examining Eq. (2), this could only come about if the value of $C_{\rm ox}$ used were lower than the measured value. In fact, to explain the fall in cross section for the $(0/-)$level in Fig. 8 would require that $C_{\rm ox}$ were 20 pF lower than the actual measured accumulation capacitance, whereas the error in $C_{\rm ox}$ was highly unlikely to be greater than 2 pF. Any error in the integration constant in Eq. (2) would only shift the measurements at each temperature on Fig. 8 up or down and would not remove the trend with Fermi energy. The fall toward the valence-band edge for the $(+/0)$ level was also likely to be real, but we cannot be quite so definite given the relatively poor quality of the p-type conductance data.

Hung and Cheng[23] have considered the effect of an energy-dependent cross section σ on the conductance peak width σ_s [i.e., $\sigma = \sigma_0 \exp(-\gamma E/k_B T)$]. Their simulations showed that a rapid change in cross section could result in significant broadening. In the data of Fig. 8 for the $(0/-)$ level at 130 K, the maximum value of Hung and Cheng's γ parameter is 0.24 which from their article would give a σ_s of 0.8. At 130 K, σ_s was already around 2 and so this broadening mechanism was not significant.

In evaluating the cross section in Fig. 8, the temperature dependence of the band gap was ignored; in addition, in the evaluation of the band bending it was assumed that the trap peak energy was not temperature dependent and so it was used to determine the integration constant in Eq. (2) for all temperatures below room temperature. This in effect amounts to treating the defect level like a shallow level composed of band-edge states so that its energy level follows the band edge. If the trap level was assumed to follow midgap (i.e., half the band-gap temperature dependence was attributed to the energy difference between the trap levels and the band edge) then the cross section was found to increase with decreasing temperature as can be seen in Fig. 9 for both types of defect for the n-type sample. The result does not appear to be particularly physically meaningful but nevertheless cannot be absolutely ruled out.

We will continue to use the assumption that the trap levels are tied to their respective band edges as in Fig. 8 and examine the cross-section data further. In addition to the energy dependence apparent in Fig. 8, there was also a significant temperature dependence. This dependence can be well reproduced by assuming the capture cross section was thermally activated, i.e,

$$\sigma = \sigma_0 \exp(-H_C/k_B T). \tag{6}$$

An Arrhenius plot of some of the P_b $(0/-)$ data from Fig. 8 is shown in Fig. 10 where it is apparent that the data were activated with an activation energy (in fact an enthalpy[21]) H_C, which increased toward the conduction-band edge. The cross-section prefactor was fairly constant, only varying between 8×10^{-20} and 2×10^{-19} m^2. In Fig. 11 the cross-section activation energy with error bars determined from the standard error of the regression fit is shown. The capture cross-section activation energy increased rapidly toward both band edges with a minimum value at the density of states peak as indicated by the arrows. This result is very similar to

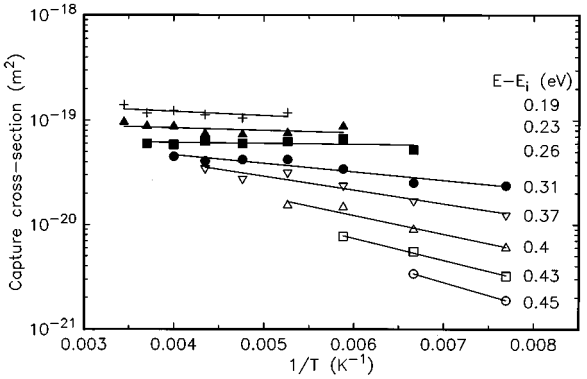

FIG. 10. Arrhenius plot of the $(0/-)$ P_b cross-section data from Fig. 8. Some biases have been omitted for clarity.

that first obtained using a capacitive transient technique by Kamieniecki *et al.*[24] They found that the capture cross section was activated and increased toward the band edge for a conventionally oxidized (100) MOS capacitor.

V. DISCUSSION

Most interface states are characterized by a continuum of levels throughout the band gap with either very broad levels or a simple U-shaped distribution rising toward the band edges. By contrast, the dangling bond levels apparent in Fig. 4 are relatively sharp but are still broader than a thermally broadened discrete level (a Fermi derivative) with the sharper level being the $(+/0)$ level closer to the valence-band edge;[9] however, the level does not show the behavior expected for a discrete level in the conductance measurement. If the level were unbroadened and were a simple discrete level, then according to Nicollian and Brews (p. 183), the conductance measurement would show a Gaussian line shape in the frequency domain as well as a Fermi derivative line shape in the density of states. In addition, the trap time constant for an electron trap is $\tau = f_D/(c_n n_S)$ where f_D is the Fermi function, n_S is the free carrier concentration, and c_n is the electron capture probability. The result of this expression for a discrete level is that the apparent capture cross section for the $(0/-)$ level measured using the conductance peak

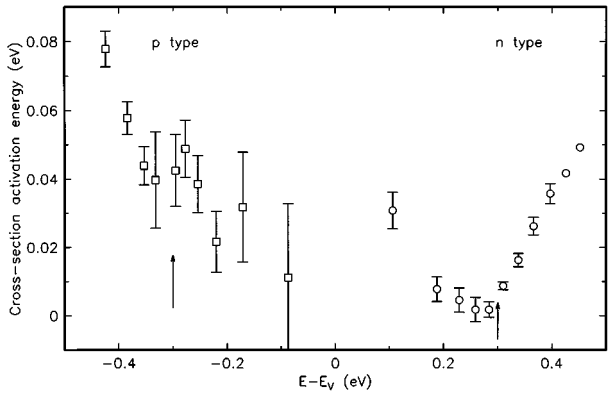

FIG. 11. Capture cross-section activation energy (enthalpy) for the data of Fig. 8 for *n*- and *p*-type capacitors.

frequency would be constant for Fermi energies below the trap level and would increase exponentially for Fermi energies above the level and closer to the conduction-band edge. This is the exact opposite of the measurements and hence it appears that there must be a distribution (continuum) of trap levels in energy.

Here we have shown that the continuum model of traps can explain the conductance peak shapes provided two contributions are taken into account. This was a five parameter fit where the second contribution at most represented about 20% of the number of defects and so it could perhaps be argued that the second contribution was an artifact that was a consequence of a systematic deviation from a Poissonian distribution of potential fluctuations. However, the extraordinarily good fit to the Nicollian and Brews model of potential fluctuations, the consistent behavior of the cross sections, and density of states as a function of energy and temperature, all lead us to believe this to be highly unlikely. Such five parameter fits to separate two defect contributions have been quite successful and reliable in the past.[14,15] The continuum model assumes that the density of states is independent of energy over at least the thermal energy of a few $k_B T/q$. This is only marginally true on the lower side of the $(0/-)$ level but is entirely reasonable on the upper side given the broad shoulder visible in Fig. 6. Assuming a continuum of levels gives potential fluctuations associated with the trapped charge which result in a broadening of 15–50 meV (Fig. 7). This broadening while significant is not sufficient to explain the asymmetric density of states that can be seen in Fig. 6.

The density of states is normally assumed to be due to the superposition of two contributions from the P_b levels superimposed on the U-shaped background.[3] Here we have separated two contributions which obey such a picture well, however, the P_b $(0/-)$ part is highly asymmetric. It is just possible that the P_b contribution could in turn be separated into two contributions with the same capture cross section; however, for this to be true, the cross sections would have to be within a factor of 2 of each other (this is because of the extremely sharp conductance peaks with σ_s values as low as 0.6 at 290 K) and show the same temperature dependence. It seems much more likely that the $(0/-)$ level is actually asymmetric.

It has been suggested[9] that the broadening is associated with the distribution of strained bonds as first measured by Brower.[8] Brower was able to fit the broadening of the EPR signal from P_b centers and found a value of 0.5° for the standard deviation of the back-bond angle to the dangling bond silicon atom at the surface. EPR measurements using the spin-dependent recombination technique which is most sensitive to defects with levels near midgap have found P_b centers, suggesting that P_b levels are distributed throughout the band gap.[25] They also found that the back-bond angle was Fermi energy dependent. Edwards[6] has calculated using a large cluster the effect of defect atom position on the P_b defect energy levels. This indicated that there was a large effect on both levels, with the defect state energy increasing as the defect atom moved closer to its nearest neighbors in a way that is consistent with Ref. 25. He also found a strong

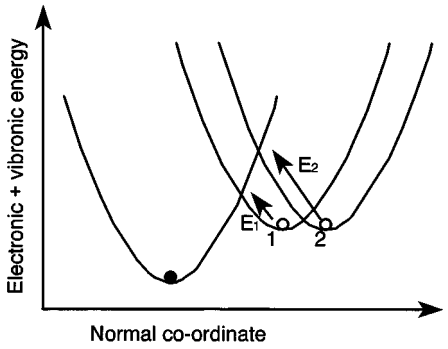

FIG. 12. Schematic configuration coordinate diagram showing the electronic plus local phonon energy for a P_b level plotted against some normal coordinate for the defect: (●) the full state; (○) two different cases of trap empty.

electron–lattice relaxation on capture, resulting in significant movement of the defect atom.

The complex behavior of the capture cross section is highly suggestive of the P_b levels showing the influence of vibronic states.[21] By contrast, the background states do not show any obvious effects. In an equilibrium measurement such as the conductance technique, the energy scale is the Gibbs free energy ($\Delta E = \Delta H - T\Delta S$), from which it follows that any entropy change on capture (ΔS) will be reflected in the apparent cross section measured. From Eq. (5), the cross section measured will be multiplied by $\exp(\Delta S/k_B)$. The fact that the apparent cross-section prefactor was roughly energy independent suggests that there was not a strong energy dependence to the entropy term. Figure 12 shows one of many possible schematic configuration coordinate diagrams for the total energy of the defect which illustrates how the measured energy dependence of the capture activation energy might arise. The parabolas represent the total energy of the defect, including the local phonon modes, for the case of trap full (solid circle) and two different cases of trap empty (open circles). It is assumed that the defect undergoes a lattice relaxation that is dependent on the field giving a horizontal shift to the parabola. Two different gate biases are then represented by the two parabolas labeled 1 and 2. It is then clear from the figure that the lattice energy needed before capture can occur (activation enthalpies for capture $E1$ and $E2$) will be strongly dependent on the degree of lattice relaxation and, hence, on Fermi energy. Such a bias-dependent lattice relaxation was inferred from EPR in Ref. 25.

VI. CONCLUSIONS

In this article we report the first detailed conductance measurements of the P_b dangling bond defect center at the (111) Si/SiO_2 interface, concentrating on the $(0/-)$ level. Temperature-dependent measurements have shown that the conductance from $(0/-)$ level is well described in terms of a continuum distribution of energy levels rather than a single discrete level. The conductance peak obeyed the potential fluctuation model of Brews exceptionally well with peak widths as narrow as $\sigma_s = 0.6$ being observed. It was possible to use the potential fluctuation model to unequivocally confirm that the upper level was an acceptor, i.e., $(0/-)$. The use of vacuum annealing to generate the P_b levels gave a particularly ''pure'' sample with only small contributions from other defects. Nevertheless, the density of states was directly separated into a contribution from the P_b $(0/-)$ center and a U-shaped background which rose toward the conduction-band edge. The $(0/-)$ density of states was found to be highly asymmetric with a large shoulder on the conduction-band side of the peak. The capture cross section for the $(0/-)$ level was found to fall toward the conduction-band edge and could be interpreted as being due to an activated capture cross section with an activation energy which increased toward the band edge. This activated capture cross section suggested strongly that lattice-relaxation effects are important for the capture kinetics of P_b centers.

ACKNOWLEDGMENTS

We would particularly like to acknowledge helpful discussions with Dr. K. M. Brunson and Dr. V. Nayar of DRA.

APPENDIX

The fitting procedure for extracting the trap parameters used an approximate function for the conductance of a continuum of levels.[20] This function is valid over the range of broadening parameter σ_s from 0.8 to 2.7 which represents typical values found for most oxides. In this particular case, the exceptionally high trap capacitance resulted in values of σ_s as low as 0.6. Sands of Hull University and Brunson of DRA Malvern have kindly supplied additional parameters which extend the range of validity of their approximate function to cover the range from $0 < \sigma_s < 0.8$. These parameters are given below and should be used with the function described in their publication (note that b_1 and b_3 are unchanged):

$$b_2 = 2.83\sigma + 0.519, \tag{A1}$$

$$b_4 = \log_{10}(qD_{\mathrm{IT}}) + 7.10\sigma - 0.210\,04, \tag{A2}$$

$$h = 0.0841 + 0.899b_2 - 0.555b_2^2 + 0.174b_2^3 - 0.0209b_2^4. \tag{A3}$$

[1] E. H. Poindexter, Semicond. Sci. Technol. **4**, 961 (1989).
[2] N. M. Johnson, D. K. Biegelsen, M. D. Moyer, S. T. Chang, E. H. Poindexter, and P. J. Caplan, Appl. Phys. Lett. **43**, 563 (1983).
[3] E. H. Poindexter, G. J. Gerardi, M.-E. Rueckel, P. J. Caplan, N. M. Johnson, and D. K. Biegelsen, J. Appl. Phys. **56**, 2844 (1984).
[4] K. L. Brower, Appl. Phys. Lett. **43**, 1111 (1983).
[5] A. H. Edwards, Phys. Rev. B **44**, 1832 (1991).
[6] A. H. Edwards, Phys. Rev. B **36**, 9638 (1987).
[7] K. L. Brower, Semicond. Sci. Technol. **4**, 970 (1989).
[8] K. L. Brower, Phys. Rev. B **33**, 4471 (1986).
[9] E. Cartier and J. H. Stathis, Appl. Phys. Lett. **69**, 103 (1996).
[10] J. F. Conley, Jr. and P. M. Lenahan, in *The Physics and Chemistry of SiO_2 and the Si–SiO_2 Interface—3*, edited by H. Z. Massoud, E. H. Poindexter, and C. R. Helms (Electrochemical Society, Pennington, NJ, 1996), Vol. 96-1, pp. 214–249.
[11] E. Cartier and J. H. Stathis, Microelectron. Eng. **28**, 3 (1995).
[12] E. H. Nicollian and J. R. Brews, *MOS (Metal Oxide Semiconductor) Physics and Technology* (Wiley, New York, 1982).
[13] M. J. Uren, S. Collins, and M. J. Kirton, Appl. Phys. Lett. **54**, 1448 (1989).
[14] N. Haneji, L. Vishnubhotla, and T. P. Ma, Appl. Phys. Lett. **59**, 3416 (1991).

[15] M. J. Uren, K. M. Brunson, and A. M. Hodge, Appl. Phys. Lett. **60**, 624 (1992).
[16] M. J. Uren, J. M. Ostler, and A. M. Hodge, Microelectron. Eng. **28**, 11 (1995).
[17] S. M. Sze, *Physics of Semiconductor Devices* (Wiley, New York, 1981).
[18] M. J. Uren and K. M. Brunson, Semicond. Sci. Technol. **9**, 1504 (1994).
[19] M. J. Kirton and M. J. Uren, Adv. Phys. **38**, 367 (1989).
[20] D. Sands and K. M. Brunson, Solid-State Electron **37**, 383 (1994).
[21] O. Engström and H. G. Grimmeiss, Semicond. Sci. Technol. **4**, 1106 (1989).
[22] D. Sands, K. M. Brunson, and M. H. Tayarani-Najaran, Semicond. Sci. Technol. **7**, 1091 (1992).
[23] K. K. Hung and Y. C. Cheng, J. Appl. Phys. **62**, 4204 (1987).
[24] E. Kamieniecki, N. Gomma, A. Kloc, and R. Nitecki, J. Vac. Sci. Technol. **18**, 883 (1981).
[25] M. A. Jupina and P. M. Lenahan, IEEE Trans. Nucl. Sci. **NS-37**, 1650 (1990).